

Isorecticular Homochiral Porous Metal–Organic Structures with Tunable Pore Sizes

Danil N. Dybtsev,^{†‡} Maxim P. Yutkin,[†] Eugenia V. Peresyphkina,[†] Alexander V. Virovets,[†] Christian Serre,[‡] Gérard Férey,[‡] and Vladimir P. Fedin^{*†}

Nikolaev Institute of Inorganic Chemistry, Siberian Branch of the Russian Academy of Sciences, Pr. Lavrentieva 3, Novosibirsk 630090, Russia, and Institut Lavoisier, Université de Versailles Saint-Quentin-en-Yvelines, 45 Avenue des Etats-Unis, 78035 Versailles Cedex, France

Received May 13, 2007

Chiral-layered building motifs of zinc(II) camphorate are linked through linear N-donor ligands, forming series of three-dimensional isorecticular porous homochiral frameworks. The lengths of these linear ligands control the pore sizes and free accessible volumes of the homochiral metal–organic structures.

Porous metal–organic frameworks (coordination polymers) are assembled from both inorganic and organic building units, thus providing a virtually endless number of possible structures with variable properties and potential applications,^{1–3} where the gas storage^{4–8} and selective separation^{9–12} demonstrate the most promising results. Homochiral porous coordination polymers, which contain regular asymmetric centers incorporated into the metal–organic framework, are an important subclass of such materials and are believed to be the best suited for stereo-

selective catalytic activation in mild conditions.¹³ Moreover, porous homochiral structures are capable of stereoselective sorption and chiral resolution of racemic mixtures onto different enantiomers. The fine purification of chiral bioactive molecules is a very important problem, especially for pharmaceuticals, because the nature often treats pairs of enantiomers as different compounds. In spite of such demanding applications, only a few porous homochiral metal–organic frameworks possessing stereoselective catalytic activity^{14–16} or enantioselective sorption properties^{17–19} have been reported to date. One of the significant difficulties in the synthesis of porous homochiral structures is organic bridging ligands, which should be chiral, rigid, and lengthy enough to provide sufficient mechanical stability and porosity for the hybrid structure.²⁰ Recently, a novel approach for the rational synthesis of homochiral porous coordination polymers has been introduced (Scheme 1).¹⁸ The key feature of the scheme is the utilization of two organic ligands simultaneously, one of them bearing asymmetric centers and another one acting as a rigid spacer for the porosity of the metal–organic framework. In the present work, we successfully applied that very approach for the synthesis of three isorecticular homochiral porous coordination polymers, built from zinc, (+)-camphoric acid (H₂camph), and another rigid linear N-donor spacer (linker), such as diazabicyclo[2.2.2]-octane (dabco), 4,4'-bipyridyl (bipy), or *trans*-bis(4-pyridyl)ethylene (bpe). Remarkably, these metal–organic frameworks are based on the same chiral-layered secondary building motif of zinc(II) camphorate, connected via linear

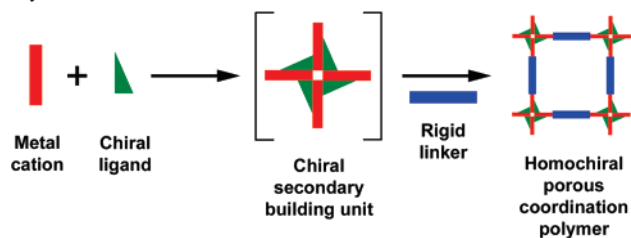
* To whom correspondence should be addressed. E-mail: cluster@che.nsk.su.

[†] Siberian Branch of the Russian Academy of Sciences.

[‡] Université de Versailles Saint-Quentin-en-Yvelines.

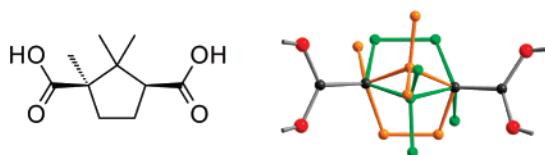
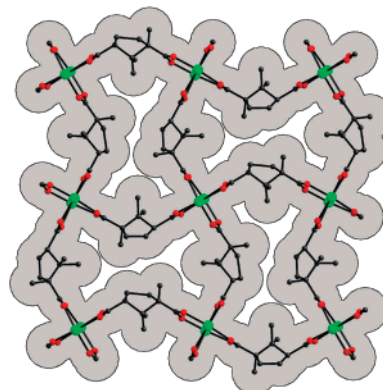
- (1) Kitagawa, S.; Kitaura, R.; Noro, S. *Angew. Chem., Int. Ed.* **2004**, *43*, 2334.
- (2) Janiak, C. *J. Chem. Soc., Dalton Trans.* **2003**, 2781.
- (3) Yaghi, O. M.; O'Keeffe, M.; Ockwing, N. W.; Chae, H. K.; Eddaoudi, M.; Kim, J. *Nature* **2003**, *423*, 705.
- (4) Férey, G.; Mellot-Draznieks, C.; Serre, C.; Millange, F.; Dutour, J.; Surblé, S.; Margiolaki, I. *Science* **2005**, *309*, 2040.
- (5) Wong-Foy, A. G.; Matzger, A. J.; Yaghi, O. M. *J. Am. Chem. Soc.* **2006**, *128*, 3494.
- (6) Eddaoudi, M.; Kim, J.; Rosi, N.; Vodak, D.; Wachter, J.; O'Keeffe, M.; Yaghi, O. M. *Science* **2002**, *295*, 469.
- (7) Chun, H.; Dybtsev, D. N.; Kim, H.; Kim, K. *Chem.—Eur. J.* **2005**, *11*, 3521.
- (8) Matsuda, R.; Kitaura, R.; Kitagawa, S.; Kubota, Y.; Belosludov, R. V.; Kobayashi, T. C.; Sakamoto, H.; Chiba, T.; Takata, M.; Kawazoe, Y.; Mita, Y. *Nature* **2005**, *436*, 238.
- (9) Dybtsev, D. N.; Chun, H.; Yoon, S. H.; Kim, D.; Kim, K. *J. Am. Chem. Soc.* **2004**, *126*, 32.
- (10) Chen, B.; Liang, Ch.; Yang, J.; Contreras, D. S.; Clancy, Y. L.; Lobkovsky, E. B.; Yaghi, O. M.; Dai, Sh. *Angew. Chem., Int. Ed.* **2006**, *45*, 1390.
- (11) Pan, L.; Olson, D. H.; Ciemnomolonski, L. R.; Heddy, R.; Li, J. *Angew. Chem., Int. Ed.* **2006**, *45*, 616.
- (12) Uemura, K.; Kitagawa, S.; Fukui, K.; Saito, K. *J. Am. Chem. Soc.* **2004**, *126*, 3817.

- (13) Davis, M. E. *Nature* **2002**, *417*, 813.
- (14) Seo, J. S.; Wand, D.; Lee, H.; Jun, S. I.; Oh, J.; Jeon, Y.; Kim, K. *Nature* **2000**, *404*, 982.
- (15) Wu, C.-D.; Hu, A.; Zhang, L.; Lin, W. *J. Am. Chem. Soc.* **2005**, *127*, 8940.
- (16) Cho, S.-H.; Ma, B.; Nguyen, S. T.; Hupp, J. T.; Albrecht-Schmitt, Th. E. *Chem. Commun.* **2006**, 2563.
- (17) Xiong, R.-G.; You, X.-Z.; Abrahams, B. F.; Xue, Z.; Che, C.-M. *Angew. Chem., Int. Ed.* **2001**, *40*, 4422.
- (18) Dybtsev, D. N.; Nuzhdin, A. L.; Chun, H.; Bryliakov, K. P.; Talsi, E. P.; Fedin, V. P.; Kim, K. *Angew. Chem., Int. Ed.* **2006**, *45*, 916.
- (19) Bradshaw, D.; Prior, T. J.; Cussen, E. J.; Claridge, J. B.; Rosseinsky, M. J. *J. Am. Chem. Soc.* **2004**, *126*, 6106.
- (20) Kesanli, B.; Lin, W. *Coord. Chem. Rev.* **2003**, *246*, 305.

Scheme 1. Synthetic Approach to Homochiral Porous Coordination Polymers

rigid linkers (dabco, bipy, or bpe) into three-dimensional (3D) non-interpenetrated nets. Thus, the pore sizes in these structures depend on the linear ligand and could be adjusted by its length. To the best of our knowledge, this series is the first example of homochiral porous coordination polymers with an isorecticular framework and tunable structural properties.

The solvothermal, one-pot reaction of zinc nitrate $Zn(NO_3)_2 \cdot 6H_2O$, (+)- H_2camph , and a linear rigid N-donor linker in a 2:2:1 ratio in a DMF solution resulted in block-shaped crystals of $[Zn_2camph_2L] \cdot xDMF \cdot yH_2O$ (where L = dabco, bipy, or bpe; DMF = *N,N'*-dimethylformamide; *x* and *y* depend on L). The structures of $[Zn_2camph_2dabco] \cdot DMF \cdot H_2O$ (**1**) and $[Zn_2camph_2bipy] \cdot 3DMF \cdot H_2O$ (**2**) were determined by single-crystal X-ray diffraction, while the structure of $[Zn_2camph_2bpe] \cdot 5DMF \cdot H_2O$ (**3**) was elucidated from powder X-ray data because of the polycrystalline nature of **3**, which prevents correction of single-crystal cell indexing. Solvate compositions of **1–3** were found from thermogravimetric analysis, elemental analysis, and IR spectroscopy. The framework stability toward guest exchange/removal was studied by means of powder X-ray diffraction and N_2 sorption measurements. According to the single-crystal X-ray analysis of **1** and **2**, the camphorate ligands are always inherently disordered over two positions (Figure 1). The primary building unit in all three metal–organic networks is a well-known binuclear “paddlewheel” zinc carboxylate complex $[Zn_2(COO)_4N_2]$ with distorted octahedral geometry of inner-sphere ligands. These Zn_2 units are connected in two dimensions via rigid chiral camphorate dicarboxylic bridges into infinite planar layers of zinc(II) camphorate $\{Zn_2camph_2\}$ having square-grid topology (Figure 2). Such layered homochiral motifs $\{Zn_2camph_2\}$ are essentially similar in all three compounds **1–3** and apparently could be regarded as secondary building units. The linear N-donor ligands (dabco, bipy, and bpe) are coordinated to the Zn^{2+} cations, perpendicularly to these $\{Zn_2camph_2\}$ layers, thus linking them and forming scaffold-like 3D metal–organic structures **1–3**, respectively, with primitive cubic (α -Po) topology. Recently, several research groups have reported a number of isorecticular metal–organic structures with the

**Figure 1.** Schematic drawing of H_2camph (left) and a typical structure of its disorder (right) over two positions (green and orange). The ordered part is shown gray.**Figure 2.** Structure of the layered motif $\{Zn_2camph_2\}$. Only one position of the disordered (+)-camphorate anion is shown. Legend: Zn, green; O, red; C, gray. The light-gray color outlines van der Waals radii of the framework atoms, indicating the density of the ligand packing.

same topology, based on such “paddlewheel” motifs.^{21–26} In our case, there is a notable difference in the structure of the dicarboxylic bridging ligand because H_2camph is intrinsically bent, compared to widely used linear dicarboxylates, like terephthalate, etc. This results in a severely distorted pattern of $\{Zn_2camph_2\}$ layers, where each cell resembles a squeezed (biconcave) circle, and quite a tight packing of camph ligands in the $\{Zn_2camph_2\}$ layer (Figure 2). As the positive outcome, such packing prevents any framework interpenetration so the metal–organic polymeric structures **1–3** are all comprised of single nets, although the drawback is hampered access to chiral centers of the camph ligands for a potential enantioactive substrate.

The linear N-donor linkers are coordinated to the Zn^{2+} cations, connecting the neighboring $\{Zn_2camph_2\}$ -layered secondary building units together. Thus, the interlayer distances are solely controlled by the lengths of these N-donor bridges. Interestingly, the layer stacking mode in the structures **1** and **2** is different. In **1**, the layers of $\{Zn_2camph_2\}$ are situated exactly atop of each other and hence have AAAA type of packing. At the same time, in **2** the layers alternate, obeying ABAB law (Figure 3). As a result, the structures **1** and **2** must be refined in different space groups: primitive $P4_21_2$ for **1** and face-centered $F222$ for **2**. In order to establish the structure of **3**, we simulated its X-ray powder pattern for both primitive and face-centered space groups, assuming that **3** has the same layered chiral secondary building blocks $\{Zn_2camph_2\}$ interlinked by bpe linear ligands and isorecticular α -Po topology of the 3D net. Interestingly, the experimental diffraction pattern of **3** has very good coincidence in general and combines the features of both types of layer packing (see the Supporting Information). This means that **3** is very likely composed of $\{Zn_2camph_2\}$ chiral layers, connected via bpe linkers, as we proposed, but the packing modes of these layers are irregular. In turn, this results in the polycrystalline nature of the

(21) Dybtsev, D. N.; Chun, H.; Kim, K. *Angew. Chem., Int. Ed.* **2004**, *43*, 5033.

(22) Seki, K.; Mori, W. *J. Phys. Chem. B* **2002**, *106*, 1380.

(23) Kitaura, R.; Iwahori, F.; Matsuda, R.; Kitagawa, S.; Kubota, Y.; Takata, M.; Kobayashi, T. C. *Inorg. Chem.* **2004**, *43*, 6522.

(24) Ma, B.-Q.; Mulfort, K. L.; Hupp, J. T. *Inorg. Chem.* **2005**, *44*, 4912.

(25) Cotton, F. A.; Lin, Ch.; Murillo, C. A. *Acc. Chem. Res.* **2001**, *34*, 759.

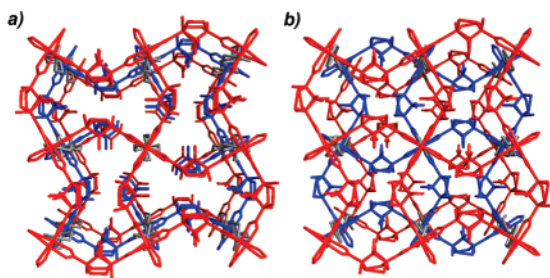


Figure 3. Perspective view along the *c* axis at the structures **1** (a) and **2** (b), showing the differences of the $\{Zn_2camph_2\}$ layer packing mode. Alternating layers are red and blue; linear N-donor ligands are gray. Guest molecules and some disordered positions are omitted.

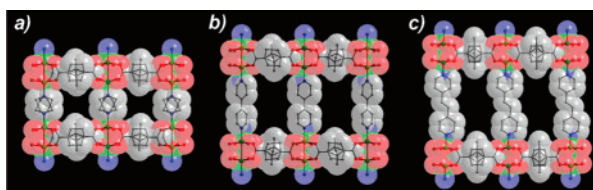


Figure 4. Side view of the metal–organic framework structures $[Zn_2\text{-camph}_2\text{dabco}]$ (a), $[Zn_2\text{camph}_2\text{bipy}]$ (b), and $[Zn_2\text{camph}_2\text{bpe}]$ (c). Camphorate ligands are shown as disordered. Some disordered atoms of N-donor linkers are removed for clarity. Legend: Zn, green; O, red; N, blue; C, gray.

crystals, which is always observed in the single-crystal X-ray experiments for **3**. Consequently, the three porous metal–organic frameworks **1–3** are built from the same chiral-layered motif $\{Zn_2camph_2\}$ linked by the linear bridges into a porous 3D net with the primitive cubic topology. Except for the minor differences in the packing modes of the layers, these structures could be considered isotypical. More importantly, the structural features of these frameworks (interlayer distances, pore sizes, and free volumes) are controlled by the lengths of the N-donor ligands. Thus, the calculated guest accessible free volumes for the metal–organic frameworks **1–3** were found to be 31, 49, and 55% respectively,²⁷ which is in the perfect correlation with the linker length increase from dabco (4.5 Å) to bipy (8.0 Å) and bpe (10.5 Å). In the same way, the free sizes of the intersecting channels vary from 3×3.5 Å for **1** to 5×7 Å for **2** and 5×10 Å for **3** (Figure 4). The inner microporous space of metal–organic hosts **1–3** is occupied by guest solvent DMF and water molecules. Because of the high crystal symmetry and intrinsic disorder, we were not able to locate these guest molecules, so the composition of as-synthesized **1–3** was established from thermogravimetric analysis weight loss and elemental analysis. The found increasing number of guest molecules (DMF + H₂O in **1**, 3DMF + H₂O in **2**, 5DMF + H₂O in **3**) per formula unit $[Zn_2camph_2L]$ is also in good agreement with the structural features of the corresponding compounds. To our best knowledge, the structures **1–3** represent the first example of a series of homochiral coordination polymers with isorecticular porous frameworks and adjustable structural features.

In order to establish the framework stability in **1–3**, the corresponding as-synthesized crystalline materials were

heated in vacuo for 1 day at 120 °C. The evacuated powders were examined by X-ray diffraction, which shows rigidity for the guest-free metal–organic structure in **1** and collapse of the host frameworks in **2** and **3** (see the Supporting Information). The permanent porosity of $[Zn_2camph_2dabco]$ was further supported by the N₂ sorption isotherm, which shows a reversible type I curve, characteristic of microporous materials with a Langmuir surface area of 553 cm³/g. At the same time, there was no N₂ sorption observed for the evacuated samples of **2** and **3**. Nevertheless, the permanent porosity and high structural rigidity is not an obligatory feature for the homochiral porous materials because they are expected to be utilized mostly in mild conditions and liquid media. In that case, the framework structure in **2** is maintained during the room-temperature reversible guest exchange to CH₂Cl₂ and back to DMF. Also, the framework integrity in **2** was additionally supported because the corresponding amorphous evacuated sample $[Zn_2camph_2bipy]$ restores its original structure after immersion in DMF for 3 days since we noticed no significant differences in X-ray powder patterns between as-synthesized and guest-reexchanged structures for **2**. In turn, structure **3** with the longest linker bpe seems to collapse during the above-mentioned guest exchange. Also, amorphous guest-free sample $[Zn_2camph_2bpe]$ does not restore the crystallinity after soaking in DMF. The corresponding X-ray powder patterns, illustrating the guest-dependent transformations of **1–3**, could be found in the Supporting Information. Such a different behavior and stability of polymeric metal–organic host structures in **1–3** could be classified according to their framework dynamics.²⁸ Thus, the framework **3** is a first-generation material, showing irreversible collapse of the framework upon guest removal. The robust, permanently porous structure **1** is a typical second-generation material, while structure **2** is a third-generation coordination polymer featuring reversible guest-dependent changes of the porous metal–organic framework.

In conclusion, we demonstrate here for the first time a simple one-pot synthesis of a series of three homochiral porous coordination polymers from enantiopure H₂camph and other readily available starting compounds. These non-interpenetrated isorecticular structures share the same chiral-layered secondary building units interlinked by rigid linear ligands, which control the important structural properties, such as the pore sizes and the free accessible volumes. The stability of the metal–organic frameworks depends on the length and nature of the linear linker.

Acknowledgment. The authors acknowledge the Russian Foundation for Basic Research (Grants 05-03-32126 and 07-03-91208) and INTAS (Grant 05-109-5007 for D.N.D.).

Supporting Information Available: Detailed description of experimental procedures, X-ray crystallographic information for **1** and **2**, powder X-ray diffraction patterns, spectroscopic data, and gas sorption data as PDF and CIF files. This material is available free of charge via the Internet at <http://pubs.acs.org>.

IC7009226

(26) Chen, B.; Ma, S.; Zapata, F.; Lobkovsky, E. B.; Yang, J. *Inorg. Chem.* **2006**, *45*, 5718.

(27) Spek, A. L. *Acta Crystallogr., Sect. A* **1990**, *A46*, C34.

(28) Kitagawa, S.; Uemura, K. *Chem. Soc. Rev.* **2005**, *34*, 109.